Available online at www.qu.edu.iq/journalcm
JOURNAL OF AL-QADISIYAH FOR COMPUTER SCIENCE AND MATHEMATICS
ISSN:2521-3504(online) ISSN:2074-0204(print)

Effect of the Rotation and Inclined Magnetic Field on Peristaltic Slip Flow of a Bingham Fluid in Asymmetric Channel and Porous medium

Mohammed Obayes Kadhim*[a] ,Liqaa Z. Hummady*[b]

1Department of Mathematics, College of Science, University of Baghdad, Baghdad, Iraq, E-mail: m.m.96moh@gmil.com

2Department of Mathematics,College of Science,University of Baghdad, E-mail:liqqa.hummady@sc.uobaghdad.edu.iq

ARTICLEINFO

Article history:
Received: 12 /03/2023
Rrevised form: 15 /04/2023
Accepted: 19 /04/2023
Available online: 30 /06/2023

Keywords:

peristaltic flow, rotation, inclined magnetic field, Bingham Fluid, Porous medium, Slip.

ABSTRACT

This essay aims to describe the peristaltic behavior of Bingham's fluid in an asymmetric channel and porous material. The liquid is thought to flow in a porous media and be susceptible to a powerfully inclined magnetic field. The long wavelength dependency and low Reynolds number result in a major simplification of the nonlinear equations. The pressure gradient, pressure rise per wavelength, axial velocity, spin velocity, volume flow rate, and tilted magnetic number are all given specific attention. The findings reveal that rotation, density, permeability, coupling diversity, and non-dimensional wave amplitude all play significant roles in the phenomenon. With rising slip coefficient values and falling magnetic field strengths, permeability, and yield stress coefficients the trapped bolus grows in size.

MSC..

https://doi.org/10.29304/jqcm.2023.15.2.1249

1. Introduction

The peristaltic mechanism is well-studied in the realm of fluid research because it has several uses in both physiological and industrial settings. Through a progressive wave of stretching and reducing motion along the fluid-carrying tube channel, peristalsis promotes fluid flow inside the corresponding system. In biological systems, peristalsis is responsible for a variety of processes, such as the development of chyme in the gastrointestinal tract, the transport of spermatozoa in the ducts efferent of the male reproductive tract, the development of the ovum in the female fallopian tube, the Vaso-movement of little veins, the transport of the fetus in the non-pregnant uterus, and the transport of urine from the kidney to the bladder are all included. Inappropriate peristalsis is the main factor contributing to the sterility of the human uterus, the thrombus improvement of blood, and the neurotic passage of microscopic organisms [1]. A fluid has the ability to flow

∗Corresponding author Mohammed Obayes Kadhim , Liqaa Z. Hummady

Email addresses: m.m.96moh@gmil.com , liqqa.hummady@sc.uobaghdad.edu.iq

Communicated by ‘sub etitor’ alaa Taima Al-Daoudi

regardless of its size. Gases and liquids are both fluids, and each is characterized by a "State Equation" that ties stress to strain rate. Breathing, blood flow, swimming, pumps, fans, turbines, airplanes, and ships are all examples of fluid engineering applications. Almost everything on our world is a fluid or moves with relation to a fluid, if you think about it. Fluid mechanics is an area of applied mathematics that examines the dynamics of fluids in motion (fluid dynamics) or at rest (fluid statics) [2]. Narahari and Sreenadh [3] To comprehend the peristaltic behavior of a Newtonian fluid in contact with a Bingham fluid, two-layer fluid models were examined. To examine the flow behavior in the unyielded plug area. Mekheimer [4] investigated how a generated magnetic field affected a magneto micropolar fluid's peristaltic flow. Pandey and Chaube [5] also investigated how an external magnetic field affected the peristaltic flow of a micropolar fluid through a porous medium. Setting exposure limits for these devices requires evaluating the impact of magnetic fields on physiological systems. The peristaltic flow of blood has been demonstrated to be greatly influenced by magnetic fields because erythrocytes, a significant portion of blood, are known to have bio magnetic properties. Due to this, efforts have been made to provide an explanation for why fluid undergoes peristalsis when subjected to magnetic fields. Abdulsalam et al. [6] examined the effects of a magnetic field on the peristaltic mechanism of an electrically conducting hyperbolic tangent fluid when applied with ion and hall slip. By utilizing the perturbation method, Hayat et al. [7] have focused on the peristaltic flow of Maxwell fluid in an asymmetric channel. Abd El Naby et al. [8] examined the effect of an attractive field on peristaltic catching to collect Newtonian liquid in a conduit. [9]describes the peristaltic behavior of a fluid in the Bingham equation with variable viscosity under the premise that the fluid is subject to a magnetic field with a significant inclination and flows within a porous medium. In [10], authors investigated the effect the rotation and initial stress on the peristaltic flow of an incompressible fluid. investigating the inclination effects of magnetic field and rotation on peristaltic slip flow of a Bingham fluid is the goal of the current study. The influence of heat and mass transfer on peristaltic transport of viscoelastic fluid in presence of magnetic field through symmetric channel with porous medium has been investigated [11]. Investigating the inclination effects of magnetic field and rotation on peristaltic slip flow of a Bingham fluid is the goal of the current study. Low Reynolds number and long wavelength assumptions are used. Axial velocity, spin velocity, stream function, and pressure rise per wavelength have exact formulas that are produced. Pictures have been used to highlight the relevant restrictions.

2. Mathematic Formulation

In a non-uniform asymmetric channel with a porous medium, consider the two-dimensional flow of a Bingham fluid. Flow results from sinusoidal wave trains moving at a steady pace along the elastic channel walls (see Fig. A). The proposed cause of the channel wall deformation is

$$\overline{h_1}(\bar{x},\bar{t}) = E_1 - r_1 \sin[\frac{2\pi}{\lambda}(\bar{x} - c\bar{t})] \quad \text{upper wall,} \tag{1}$$

while at the lower wall is given by.

$$\overline{h_2}(\bar{x},\bar{t}) = -E_2 - r_2 \sin[\frac{2\pi}{\lambda}(\bar{x} - c\bar{t}) + \emptyset] \quad \text{lower wall.} \tag{2}$$

where (r_1) and (r_2) indicate the wave's amplitudes, (E_1) and (E_2) denotes the channel's width, (λ) specifying the wavelength, The direction of the wave's propagation is represented by ($\bar{X}$), while the time is indicated by ($\bar{t}$). The difference in phase ($\emptyset$) varies across the range ($0 \le \emptyset \le \pi$) in which ($\emptyset = 0$) is equivalent to an out-of-phase, asymmetric channel and ($\emptyset = \pi$) stands for the phase of the waves. Further (r_1), (r_2), (E_1), (E_2), and ($\emptyset$) satisfy the condition ($\overline{h_1}(\bar{x},\bar{t}) = H_1$, $\overline{h_2}(\bar{x},\bar{t}) = H_2$):

$$r_1^2 + r_2^2 + 2r_1 r_2 \cos(\emptyset) \le (E_1 + E_2)^2. \tag{3}$$

Furthermore, it is assumed that the walls don't move longitudinally. This assumption limits the ability of the walls to deform rather than implying that the channel is stiff during longitudinal motions.

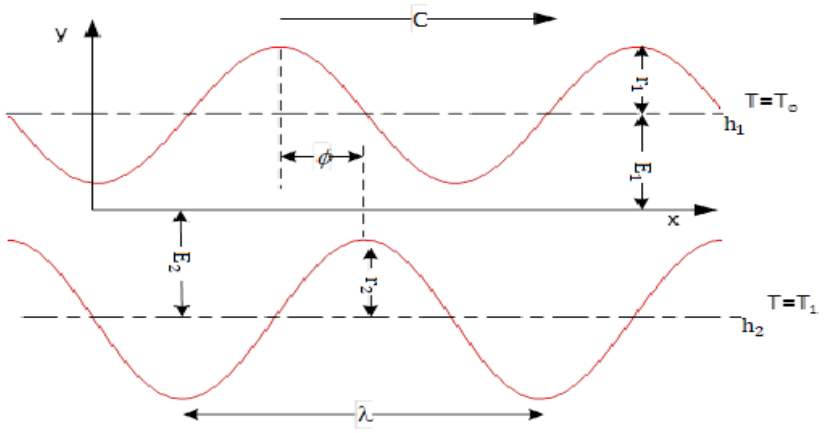

Fig. A The flow geometry

$x = X - ct$, $y = Y$, $u = U - c$, $v = V$ and $p(x, y) = P(X, Y, t)$ (4)

In the fixed and wave frames, the transverse velocity components are, respectively. These are the equations that control fluid flow in the wave frame.

$$\frac{\partial U}{\partial X} + \frac{\partial V}{\partial Y} = 0 \tag{5}$$

The $\bar{x}$ – part of the moment equation is:

$$\rho\left(\frac{\partial}{\partial \bar{t}} + \bar{u}\frac{\partial}{\partial \bar{x}} + \bar{v}\frac{\partial}{\partial \bar{y}}\right)\bar{u} - \rho\Omega\left(\Omega\bar{u} + 2\frac{\partial \bar{v}}{\partial \bar{t}}\right) = -\frac{\partial \bar{p}}{\partial \bar{x}} + \frac{\partial}{\partial \bar{x}}\bar{s}_{\bar{x}\bar{x}} + \frac{\partial}{\partial \bar{y}}\bar{s}_{\bar{x}\bar{y}} - \sigma B_0{}^2\cos\beta^*(\bar{u}\cos\beta^* - \bar{v}\sin\beta^*) - \frac{\mu}{\bar{k}}\bar{u} \tag{6}$$

The $\bar{y}$ – part of the moment equation is:

$$\rho\left(\frac{\partial}{\partial \bar{t}} + \bar{u}\frac{\partial}{\partial \bar{x}} + \bar{v}\frac{\partial}{\partial \bar{y}}\right)\bar{v} - \rho\Omega\left(\Omega\bar{v} + 2\frac{\partial \bar{u}}{\partial \bar{t}}\right) = -\frac{\partial \bar{p}}{\partial \bar{x}} + \frac{\partial}{\partial \bar{x}}\bar{s}_{\bar{x}\bar{y}} + \frac{\partial}{\partial \bar{y}}\bar{s}_{y\bar{y}} - \sigma B_0{}^2\cos\beta^*(\bar{u}\cos\beta^* - \bar{v}\sin\beta^*) - \frac{\mu}{\bar{k}}\bar{v} \tag{7}$$

The fluid exhibits behavior consistent with the Bingham model, and the following information about its Cauchy stress tensor is given

$$\sigma = -PI + \bar{S} \tag{8}$$

$$\bar{S} = 2\mu\tau + 2\tau_0\hat{\tau} \tag{9}$$

in equation (9) τ_0 is the yield stress, and the tensor of rate of deformation τ and $\hat{\tau}$ is the tensor is described:

$$\hat{\tau} = \frac{\tau}{\sqrt{2\,tras\,\tau^2}} \tag{10}$$

$$\tau = \frac{1}{2}\left(\nabla\bar{V} + (\nabla\bar{V})^T\right) \tag{11}$$

where (I) Identifier Tensor, $\bar{\nabla}=(\partial\bar{X}, \partial\bar{Y}, 0)$ the gradient vector, ($\bar{P}$) the liquid's pressure and (μ) the dynamic viscosity .

$$\bar{s}_{\bar{x}\bar{x}} = 2\mu\bar{u}_{\bar{x}} + \frac{2\tau_0\bar{u}_{\bar{x}}}{\sqrt{2\bar{u}_{\bar{x}}{}^2 + \left(\bar{v}_{\bar{x}} + \bar{u}_{\bar{y}}\right)^2 + 2\bar{v}_{\bar{y}}{}^2}} \tag{12}$$

$$\bar{s}_{\bar{x}\bar{y}} = \mu\left(\bar{v}_{\bar{x}} + \bar{u}_{\bar{y}}\right) + \frac{\tau_0\left(\bar{v}_{\bar{x}} + \bar{u}_{\bar{y}}\right)}{\sqrt{2\bar{u}_{\bar{x}}{}^2 + \left(\bar{v}_{\bar{x}} + \bar{u}_{\bar{y}}\right)^2 + 2\bar{v}_{\bar{y}}{}^2}} \tag{13}$$

$$\bar{s}_{\bar{y}\bar{y}} = 2\mu\bar{v}_{\bar{y}} + \frac{2\tau_0\bar{v}_{\bar{y}}}{\sqrt{2\bar{u}_{\bar{x}}{}^2 + \left(\bar{v}_{\bar{x}} + \bar{u}_{\bar{y}}\right)^2 + 2\bar{v}_{\bar{y}}{}^2}} \tag{14}$$

The non-dimensional quantities and parameters used in the governing equations above include

$$x = \frac{1}{\lambda}\bar{x}\,,\ y = \frac{1}{E_1}\bar{y}\,,\ u = \frac{1}{c}\bar{u}\,,\ v = \frac{1}{\delta\, c}\bar{v}\,,\ t = \frac{c}{\lambda}\bar{t}\,,\ \delta = \frac{E_1}{\lambda}\,,\ Re = \frac{\rho\, c\, E_1}{\mu},\ Da = \frac{\bar{k}}{d^2}\,,\ \eta = \frac{\Omega^2 {E_1}^2 \rho}{\mu},$$

$$s_{xx} = \frac{\lambda}{\mu\, c}\bar{s}_{\bar{x}\bar{x}}\,,\ s_{xy} = \frac{E_1}{\mu\, c}\bar{s}_{\bar{x}\bar{y}}\ ,\ s_{yy} = \frac{E_1}{\mu\, c}\bar{s}_{\bar{y}\bar{y}}\ h_1 = \frac{1}{E_1}\overline{h_1}\ ,\quad h_2 = \frac{1}{E_1}\overline{h_2}\,,\ R_n = \frac{\tau_0 E_1}{\mu c}\,,\ p = \frac{{E_1}^2}{\lambda\mu\, c}\bar{p}\,. \tag{15}$$

$$\frac{\partial u}{\partial x} + \frac{\partial v}{\partial y} = 0 \tag{16}$$

$$Re\,\delta\left(\frac{\partial u}{\partial t} + u\frac{\partial u}{\partial x} + v\frac{\partial u}{\partial y}\right) - \frac{\rho d^2}{\mu}\Omega^2 u - (2\Omega\delta^2 Re)\left(\frac{\partial v}{\partial t}\right) = -\frac{\partial p}{\partial x} + \delta^2\frac{\partial}{\partial x}s_{xx} + \frac{\partial}{\partial y}s_{xy} - (Ha)^2\cos\beta^*\,(u\cos\beta^* - \delta v\sin\beta^*) - \frac{1}{Da}u \tag{17}$$

$$Re\,\delta^3\left(\frac{\partial v}{\partial t} + u\frac{\partial v}{\partial x} + v\frac{\partial v}{\partial y}\right) - \frac{\rho d^2}{\mu}\delta^2\Omega^2 v - (2\Omega\delta^2 Re)\left(\frac{\partial u}{\partial t}\right) = -\frac{\partial p}{\partial y} + \delta^2\frac{\partial}{\partial x}s_{xy} + \delta\frac{\partial}{\partial y}s_{yy} + (Ha)^2\sin\beta^*\,(\delta\, u\cos\beta^* - \delta^2\, v\sin\beta^*) - \delta^2\frac{1}{Da}v \tag{18}$$

$$h_1(x,t) = 1 - a\,sin(2\pi x)a = \frac{r_1}{E_1} \tag{19}$$

$$h_2(x,t) = -E_2 - b\,sin(\,2\pi x + \emptyset)E = \frac{E_2}{E_1}\ and\ b = \frac{r_2}{E_1} \tag{20}$$

$$s_{xx} = 2\delta\frac{\partial u}{\partial x} + \frac{2\delta R_n\left(\frac{\partial u}{\partial x}\right)}{\sqrt{2\delta^2\left(\frac{\partial u}{\partial x}\right)^2 + \left(\delta^2\frac{\partial v}{\partial x} + \frac{\partial u}{\partial y}\right)^2 + 2\delta^2\left(\frac{\partial v}{\partial y}\right)^2}} \tag{21}$$

$$s_{xy} = \left(\delta^2\,\frac{\partial v}{\partial x} + \frac{\partial u}{\partial y}\right) + \frac{R_n\left(\delta^2\frac{\partial v}{\partial x} + \frac{\partial u}{\partial y}\right)}{\sqrt{2\delta^2\left(\frac{\partial u}{\partial x}\right)^2 + \left(\delta^2\frac{\partial v}{\partial x} + \frac{\partial u}{\partial y}\right)^2 + 2\delta^2\left(\frac{\partial v}{\partial y}\right)^2}} \tag{22}$$

$$s_{yy} = 2\delta\frac{\partial v}{\partial y} + \frac{2\delta R_n\left(\frac{\partial v}{\partial y}\right)}{\sqrt{2\delta^2\left(\frac{\partial u}{\partial x}\right)^2 + \left(\delta^2\frac{\partial v}{\partial x} + \frac{\partial u}{\partial y}\right)^2 + 2\delta^2\left(\frac{\partial v}{\partial y}\right)^2}} \tag{23}$$

The relations establish a connection between the velocity components and stream function (ψ):

$$u = \partial\psi\ /\ \partial y, v = -\,\partial\psi/\partial x. \tag{24}$$

Substituted Eq. (24) in Eq. (16), (17), (18), (21), (22), (23) respectively,

$$\frac{\partial^2\psi}{\partial x\,\partial y} - \frac{\partial^2\psi}{\partial x\,\partial y} = 0 \tag{25}$$

$$Re\,\delta\left(\frac{\partial^2\psi}{\partial t\,\partial y} + \frac{\partial^3\psi}{\partial x\,\partial y^2} - \frac{\partial^3\psi}{\partial x\,\partial y^2}\right) - \frac{\rho d^2}{\mu}\Omega^2\frac{\partial\psi}{\partial y} - (2\Omega\delta^2 Re)\left(\frac{\partial^2\psi}{\partial t\,\partial x}\right) = -\frac{\partial p}{\partial x} + \delta^2\frac{\partial}{\partial x}s_{xx} + \frac{\partial}{\partial y}s_{xy} - (Ha)^2\cos\beta^*\left(\frac{\partial\psi}{\partial y}\cos\beta^* + \delta\frac{\partial\psi}{\partial x}\sin\beta^*\right) - \frac{1}{Da}\frac{\partial\psi}{\partial y} \tag{26}$$

$$\mathrm{Re}\,\delta^3\left(-\frac{\partial^2\psi}{\partial t\,\partial x}+\frac{\partial^3\psi}{\partial x^2\,\partial y}-\frac{\partial^3\psi}{\partial x^2\,\partial y}\right)+\frac{\rho d^2}{\mu}\delta^2\Omega^2\frac{\partial\psi}{\partial x}-(2\Omega\delta^2\mathrm{Re})\left(\frac{\partial^2\psi}{\partial t\,\partial y}\right)=-\frac{\partial p}{\partial y}+\delta^2\frac{\partial}{\partial x}s_{xy}+\delta\frac{\partial}{\partial y}s_{yy}+$$
$$(\mathrm{Ha})^2\sin\beta^*\left(\delta\frac{\partial\psi}{\partial y}\cos\beta^*+\delta^2\frac{\partial\psi}{\partial x}\sin\beta^*\right)+\delta^2\frac{1}{\mathrm{Da}}\frac{\partial\psi}{\partial x}, \quad (27)$$

$$s_{xx}=(2\delta)\frac{\partial^2\psi}{\partial x\,\partial y}+\frac{2\delta R_n\left(\frac{\partial^2\psi}{\partial x\,\partial y}\right)}{\sqrt{2\delta^2\left(\frac{\partial^2\psi}{\partial x\,\partial y}\right)^2+\left(-\delta^2\frac{\partial^2\psi}{\partial x^2}+\frac{\partial^2\psi}{\partial y^2}\right)^2+2\delta^2\left(-\frac{\partial^2\psi}{\partial x\,\partial y}\right)^2}} \quad (28)$$

$$s_{xy}=\left(-\delta^2\frac{\partial^2\psi}{\partial x^2}+\frac{\partial^2\psi}{\partial y^2}\right)+\frac{R_n\left(-\delta^2\frac{\partial^2\psi}{\partial x^2}+\frac{\partial^2\psi}{\partial y^2}\right)}{\sqrt{\delta^2\left(\frac{\partial^2\psi}{\partial x\,\partial y}\right)^2+\left(-\delta^2\frac{\partial^2\psi}{\partial x^2}+\frac{\partial^2\psi}{\partial y^2}\right)^2+2\delta^2\left(-\frac{\partial^2\psi}{\partial x\,\partial y}\right)^2}} \quad (29)$$

$$s_{yy}=-\delta\frac{\partial^2\psi}{\partial x\,\partial y}+\frac{2\delta R_n\left(\frac{\partial^2\psi}{\partial x\,\partial y}\right)}{\sqrt{\delta^2\left(\frac{\partial^2\psi}{\partial x\,\partial y}\right)^2+\left(-\delta^2\frac{\partial^2\psi}{\partial x^2}+\frac{\partial^2\psi}{\partial y^2}\right)^2+2\delta^2\left(-\frac{\partial^2\psi}{\partial x\,\partial y}\right)^2}} \quad (30)$$

The wave frames dimensionless slip boundary conditions are

$\psi=\frac{F}{2}$ at y= h_1, $\psi=-\frac{F}{2}$ at y= h_2,

$\frac{\partial\psi}{\partial y}+\beta_1\frac{\partial^2\psi}{\partial y^2}=-1$ at y= h_1, $\frac{\partial\psi}{\partial y}-\beta_1\frac{\partial^2\psi}{\partial y^2}=-1$ at y= h_2,

β_1 is the dimensionless slip parameter. (31)

3. Solution of the Problem

It is impossible to provide a precise answer for each of the random parameters involved. We take perturbation strategy to get the answer. We go beyond treating the disorder.

$$\psi=\psi_0+R_n\,\psi_1+O({R_n}^2),$$
$$F=F_0+R_nF_1+O({R_n}^2) \quad (32)$$

Substitute the terms (32) into Eq. (25)-(30), and the equations for the boundary conditions (31) ($\delta\ll1$), We can create the following system of comparable powers (Re) by equating the coefficients of the higher order components it entails because the power of (δ) is lower and inconsequential.

From Eq. (29) and Eq. (26) we get:

$$\frac{dp}{dx}=\eta\psi_y+\psi_{yyy}+R_n\,\psi_y-B_n\,\psi_y \quad (33)$$

$$\eta=\frac{(\Omega^2d^2\rho)}{\mu} \quad (34)$$

$$B_n=\mathrm{Ha}^2\cos^2\beta^*+\frac{1}{\mathrm{Da}} \quad (35)$$

From Eq. (27) we get:

$$\frac{\partial p}{\partial y}=0 \quad (36)$$

From differential of y for Eq. (33)

$$0 = \psi_{yyyy} + R_n\, \psi_{yy} - B_n \psi_{yy} + \eta \psi_{yy} \tag{37}$$

3.1 Zero Order System

When the order's terms are (R_n) are trivial in the system of zeroth order, we obtain:

$$\psi_{0yyyy} - B_n\, \psi_{0yy} + \eta\, \psi_{0yy} = 0 \tag{38}$$

Such that

$\psi_0 = F_0 / 2$, $\partial\psi_0 / \partial y = -1$ at y= h_1 and

$\psi_0 = -F_0 / 2$, $\partial\psi_0 / \partial y = -1$ at y= h_2

$$\frac{\partial\psi_0}{\partial y} + \beta_1 \frac{\partial^2\psi_0}{\partial y^2} = -1 \text{ at y= } h_1\,, \quad \frac{\partial\psi_0}{\partial y} - \beta_1 \frac{\partial^2\psi_0}{\partial y^2} = -1 \text{ at y= } h_2, \tag{39}$$

3.2 First order system

$$\psi_{1_{yyyy}} + \psi_{0yy} - B_n \psi_{1yy} + \eta\, \psi_{1_{yy}} = 0 \tag{40}$$

$$\psi_{1_{yyyy}} - B_n \psi_{1yy} + \eta\, \psi_{1_{yy}} = -\psi_{0yy} \tag{41}$$

$\psi_1 = F_1 / 2$, $\partial\psi_0 / \partial y = -1$ at y= h_1 and

$\psi_1 = -F_1 / 2$, $\partial\psi_0 / \partial y = -1$ at y= h_2

$$\frac{\partial\psi_1}{\partial y} + \beta_1 \frac{\partial^2\psi_1}{\partial y^2} = -1 \text{ at y= } h_1\,, \quad \frac{\partial\psi_1}{\partial y} - \beta_1 \frac{\partial^2\psi_1}{\partial y^2} = -1 \text{ at y= } h_2, \tag{42}$$

And by resolving the related zeroth and first order systems, you may obtain the final equation for the stream function:

$$\psi = \psi_0 + R_n\, \psi_1 \tag{43}$$

Where the functions (ψ_0, ψ_1) hefty expressions Consequently, they will be mentioned in Appendix.

$$\frac{\partial p}{\partial x} = \psi_{0yyy} + R_n \psi_{1yyy} + R_n \psi_{0yy} + {R_n}^2 \psi_{0yy} - B_n\, \psi_{0y} + \eta\psi_{0y} - B_n R_n \psi_{1y} + \eta R_n \psi_{1y} \tag{44}$$

The definition of pressure increases per wave length (Δp) is

$$\Delta p = \int_0^1 \frac{dp}{dx}\, dx. \tag{45}$$

4. Results and Discussion

To investigate the impact of physical factors like Effect of, Darcy number (Da), Hartman number (Ha), inclination of magnetic field (β^*), Rotation (Ω), Porous medium parameter (k), Material fluid parameters (Rn), Density (ρ), Viscosity (μ), pressure rise (Δp), slip coefficient (β_1), the plotted axial velocity (u), pressure rise and stream function (ψ) in figs. 1-8 are exemplified by software "MATHEMATICA".

4.1 Velocity Distribution (u)

Figure 1 demonstrate how the axial velocity (u) value can vary with respect to y for various rotational values (Ω), Darcy number (Da), Viscosity (μ), material fluid parameter (Rn), inclination of magnetic field (β^*), slip coefficient (β_1), Hartman number (Ha), and amplitude ratio ($\emptyset$). These figures show that the maximum velocity is consistently found close to the channel's center and that All instances of the velocity profiles are parabolic. Figures b, c, and f show that the axial velocity decreases as (Ha), (Rn), and (β_1) increase. Figures a, d, and g show that raising the (Da), (Ω), and (β^*) increases the axial velocity. Figures e and h the effect of ($\emptyset$) and (μ) when the speed increases, it starts decreasing at the left channel wall, then it merges with the other one in center, and then decreasing too at the right channel wall.

4.2 Pressure Rise (Δp)

Figure 2 display the various pressure increases in the wave outline's capability of volumetric stream rate for various Darcy number (Da), Rotation (Ω), material fluid parameter (Rn), Density (ρ), Hartman number (Ha) and slip coefficient (β_1). The relationship between a dimensionless mean flow rate (Q1) and a non-dimensional average pressure rises per wavelength will be illustrated in this paragraph along with variations in the relevant parameters in (Δp). Fig. c, e and h shows the effect of increasing the parameter (Ω), (β_1) and ($\emptyset$) on (ΔP) reveals that pressure rice per wave length ΔP increase in magnitude in all regions. Fig. b demonstrates that pressure increase (Δp) diminishes as (Da) In zone of increased pumping and the compounding region ($\Delta p < 0$), it is seen that pumping rises. According to Fig. a, the pumping rate increases in a retrograde region where ($\Delta p > 0$, $Q1 > 0$) and lowers in a cop umping zone where ($\Delta p < 0$, $Q1 < 0$), according to the graph. As the magnetic field (Ha) expands, the pressure rises ($\Delta p > 0$). Fig shows the pressure rice per wave length ΔP decreases in magnitude for fixed values of the (Rn). In Figures f and g There is no change in pressure when (ρ), (μ).

4.3 Trapping phenomena

An interesting component happens in peristaltic flows closed movement strains lure bolus, or the extent of fluid called bolus, in the channel tube close to the partitions, and this trapping bolus advances along the path of the wave. In figs 3 – 8 Plots of the stream lines are shown at different values. of (Ω), (Da), (Rn), (Ha), (ρ) and (β_1). Figs 3,5 and 8 It shows a shrinking of the trapped bolus when the (Ω), (Ha) and (ρ) is increased. Figs 4 and 6 the exhibits that the trapping exists in the focus of the channel, an increase in (Da) and (Rn) increases the size of bolus, as well effect of slip parameter (β_1) is shown in figure 7, A rise in (β_1) increased size of bolus.

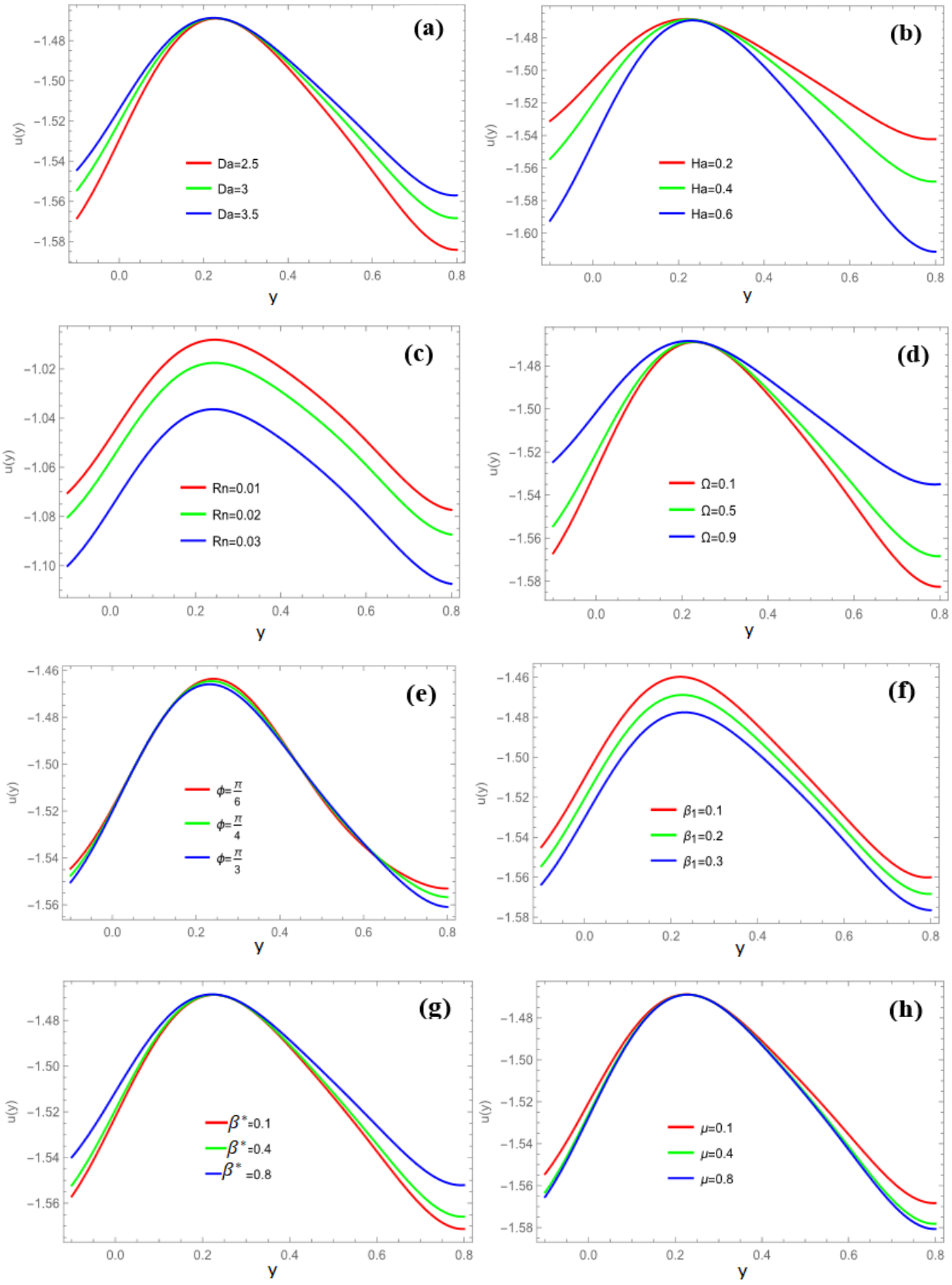

Fig. 1 Variation of Ω, Da, Ha, Rn, $\emptyset$, β_1, β^*, and μ on the axial velocity (u) with respect to y.

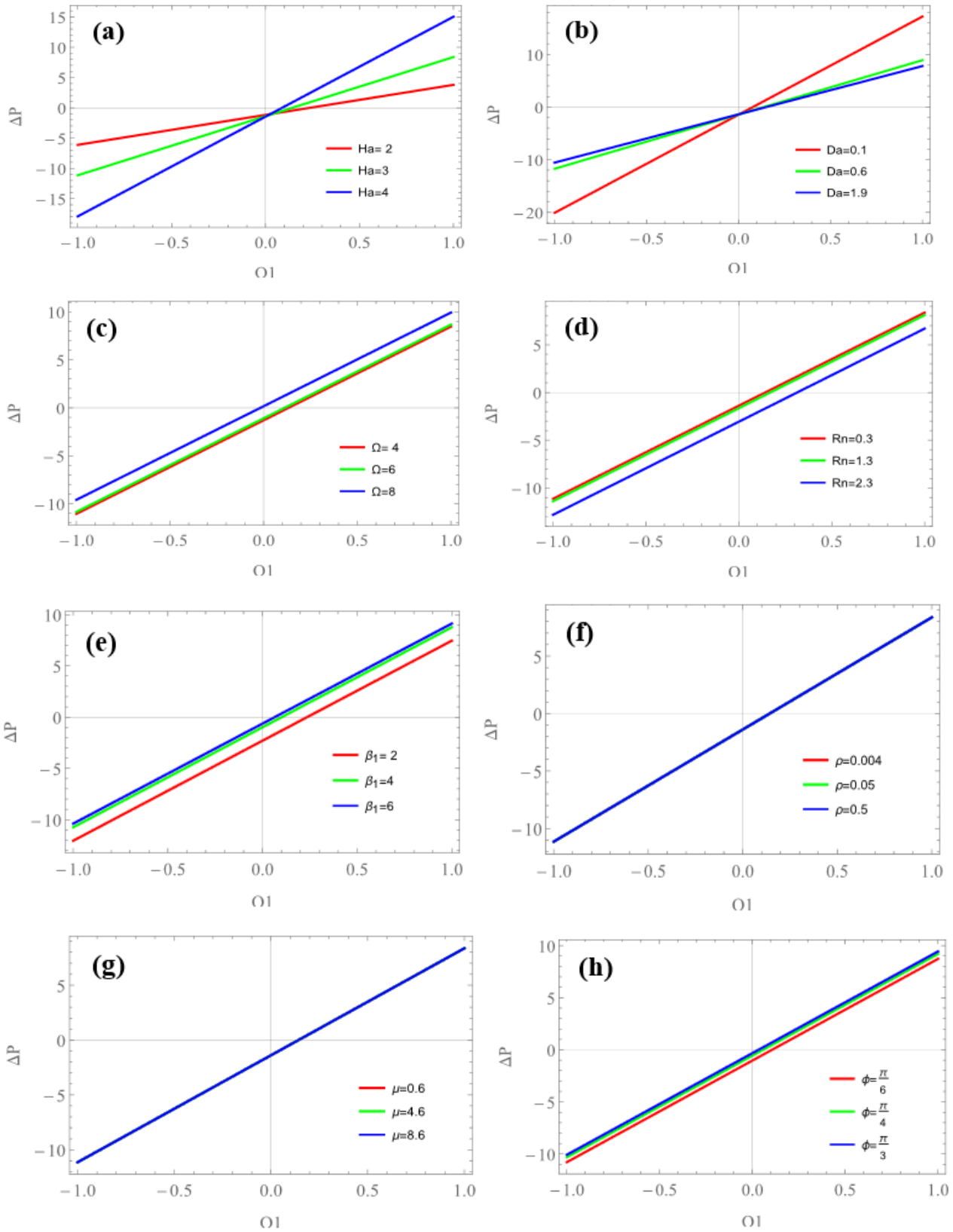

Fig. 2 Variation of Ω, Da, Ha, Rn, ∅, β_1 and μ on the pressure rise per wavelength (Δp) against the volume flow rate ˜Q

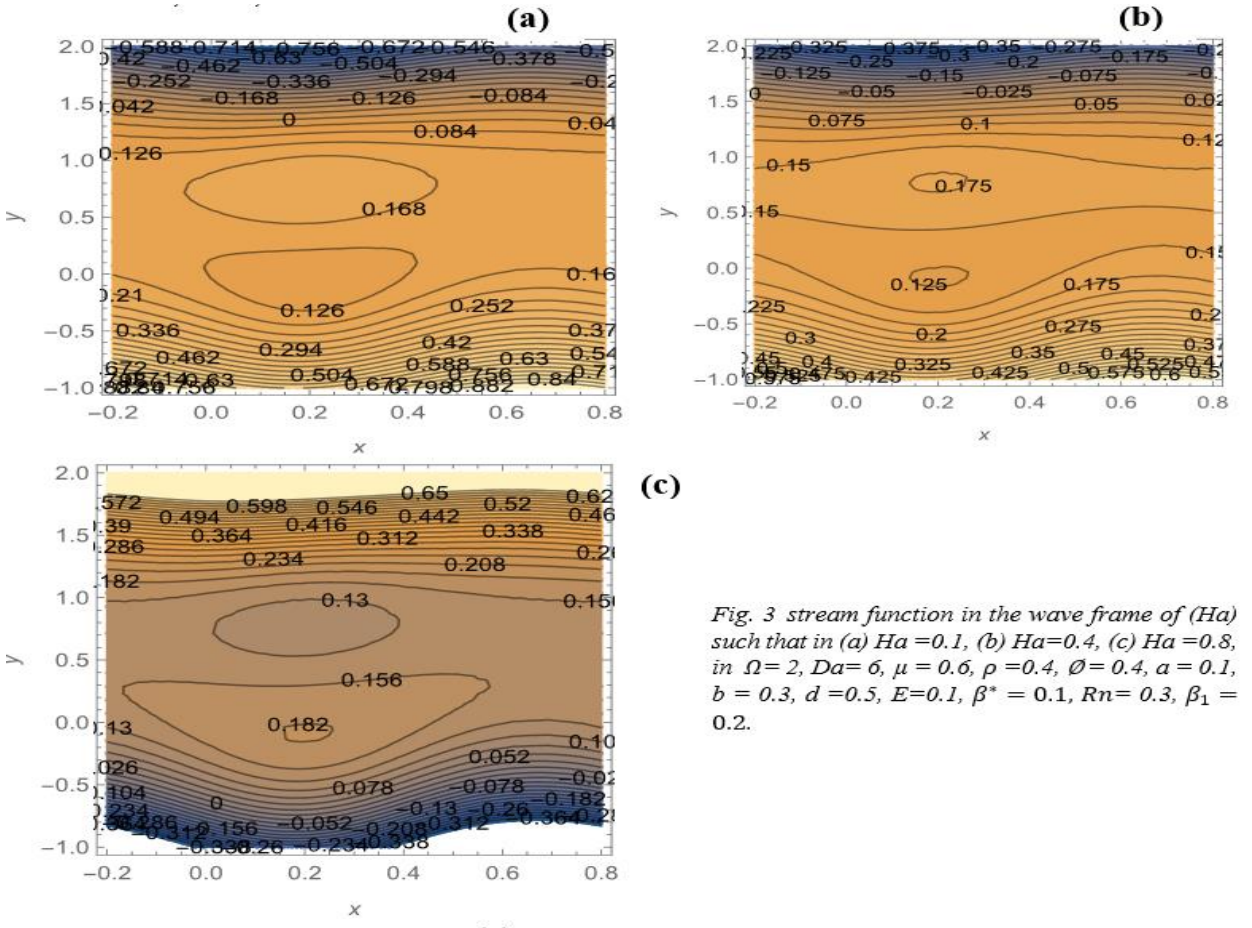

Fig. 3 stream function in the wave frame of (Ha) such that in (a) Ha =0.1, (b) Ha=0.4, (c) Ha =0.8, in Ω= 2, Da= 6, μ = 0.6, ρ =0.4, Ø= 0.4, a = 0.1, b = 0.3, d =0.5, E=0.1, β = 0.1, Rn= 0.3, β_1 = 0.2.*

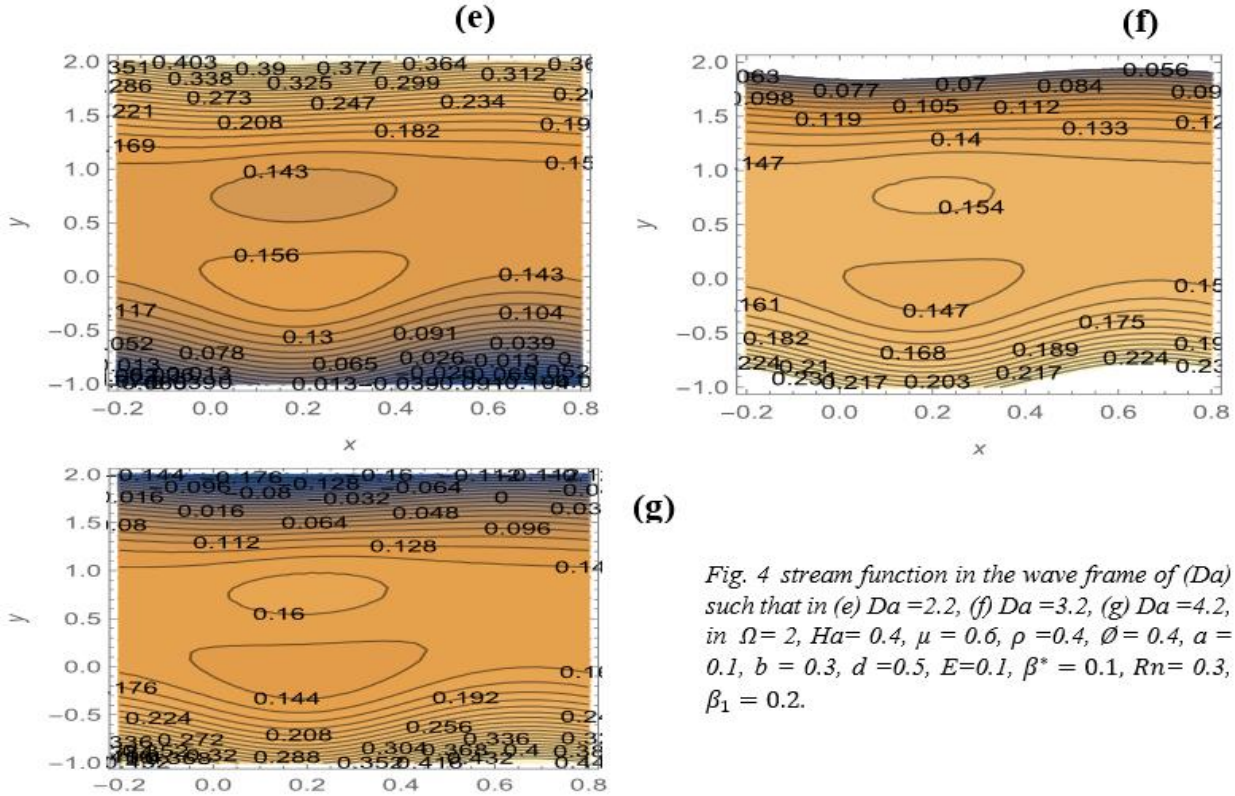

Fig. 4 stream function in the wave frame of (Da) such that in (e) Da =2.2, (f) Da =3.2, (g) Da =4.2, in Ω= 2, Ha= 0.4, μ = 0.6, ρ =0.4, Ø= 0.4, a = 0.1, b = 0.3, d =0.5, E=0.1, β = 0.1, Rn= 0.3, β_1 = 0.2.*

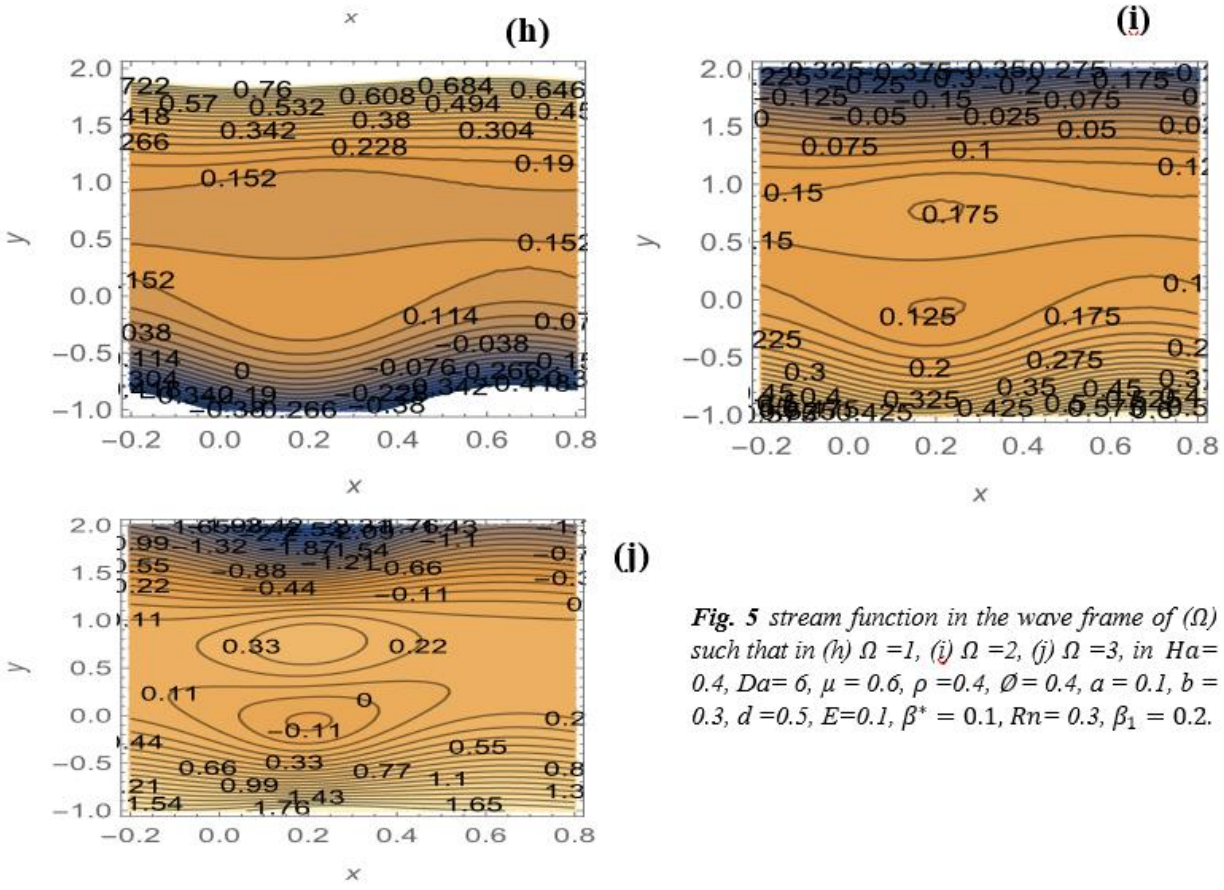

Fig. 5 *stream function in the wave frame of (Ω) such that in (h) Ω =1, (i) Ω =2, (j) Ω =3, in Ha= 0.4, Da= 6, μ = 0.6, ρ =0.4, Ø = 0.4, a = 0.1, b = 0.3, d =0.5, E=0.1, β^* = 0.1, Rn= 0.3, β_1 = 0.2.*

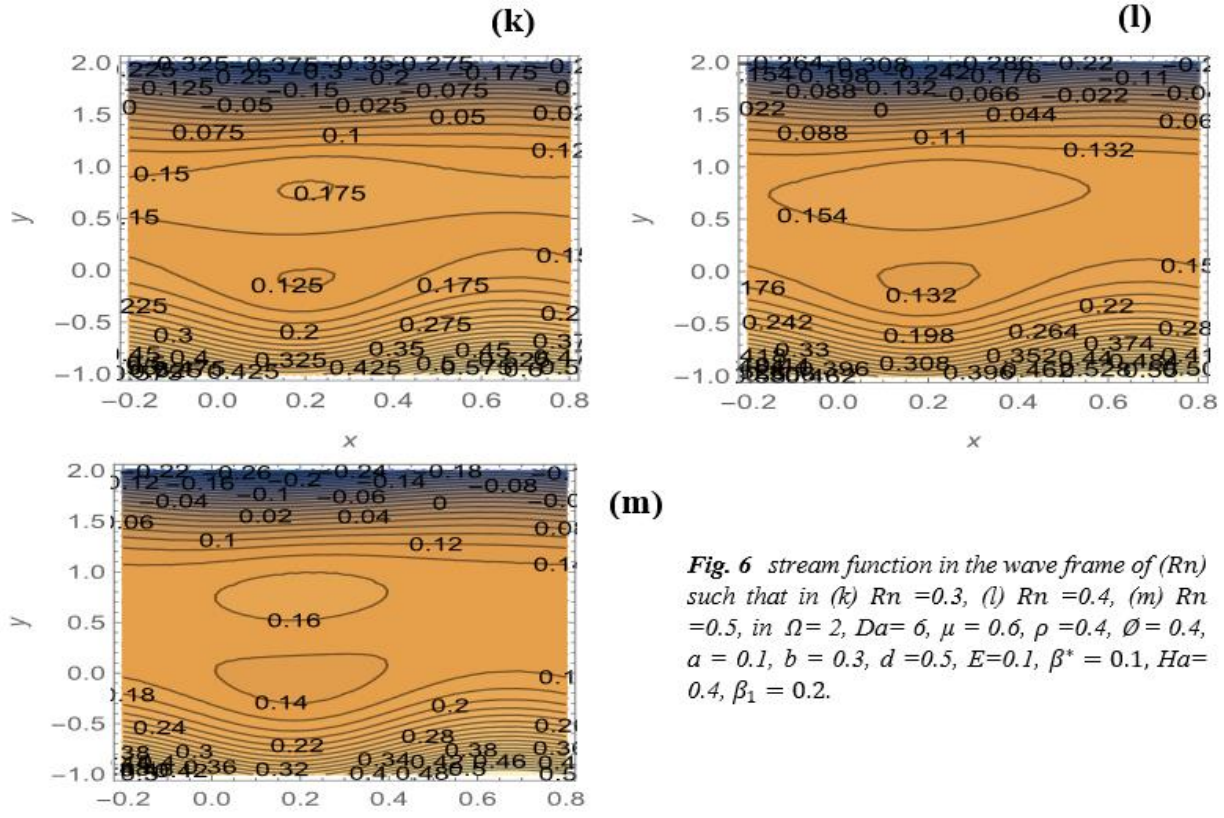

Fig. 6 *stream function in the wave frame of (Rn) such that in (k) Rn =0.3, (l) Rn =0.4, (m) Rn =0.5, in Ω= 2, Da= 6, μ = 0.6, ρ =0.4, Ø = 0.4, a = 0.1, b = 0.3, d =0.5, E=0.1, β^* = 0.1, Ha= 0.4, β_1 = 0.2.*

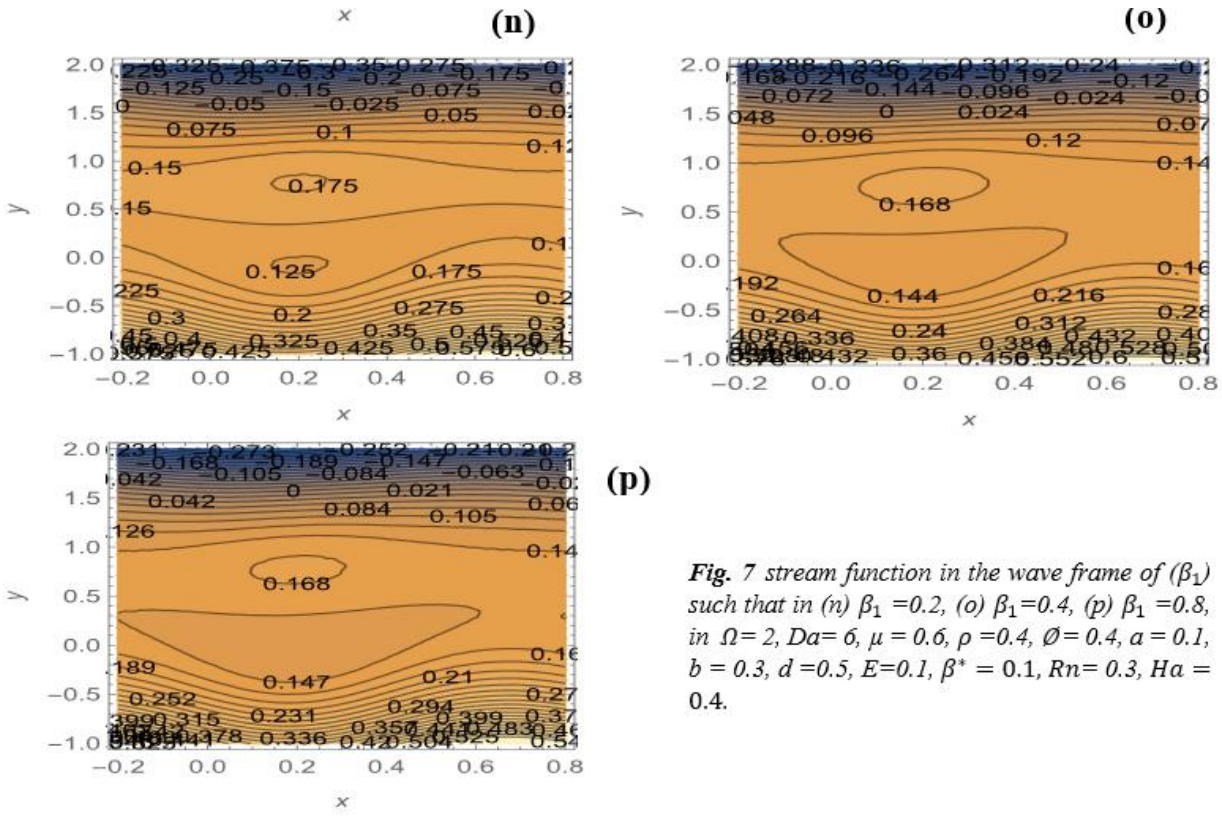

Fig. *7 stream function in the wave frame of* (β_1) *such that in (n)* β_1 *=0.2, (o)* β_1*=0.4, (p)* β_1 *=0.8, in* Ω*= 2, Da= 6,* μ *= 0.6,* ρ *=0.4,* $\emptyset$*= 0.4, a = 0.1, b = 0.3, d =0.5, E=0.1,* β^* = 0.1, *Rn= 0.3, Ha =* 0.4.

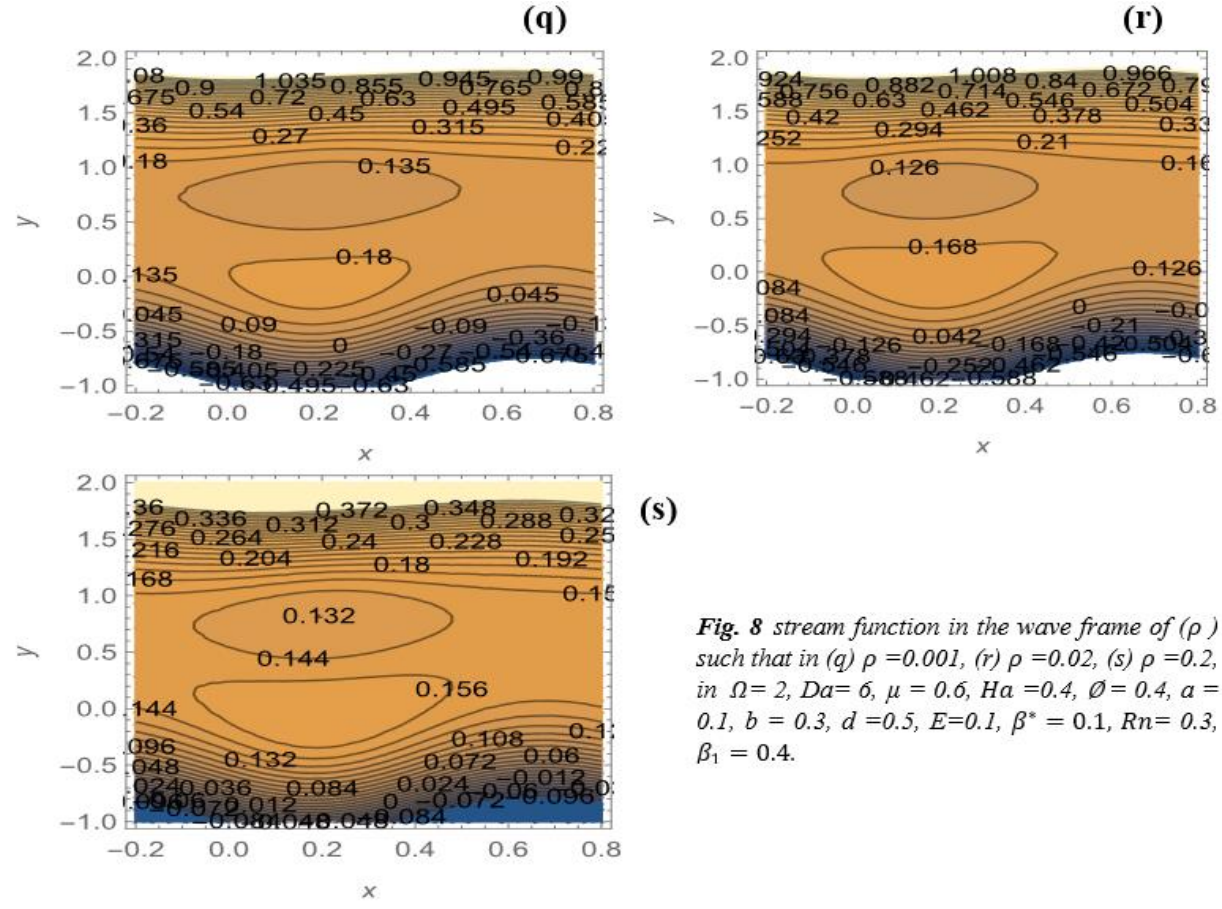

Fig. *8 stream function in the wave frame of* (ρ) *such that in (q)* ρ *=0.001, (r)* ρ *=0.02, (s)* ρ *=0.2, in* Ω*= 2, Da= 6,* μ *= 0.6, Ha =0.4,* $\emptyset$*= 0.4, a = 0.1, b = 0.3, d =0.5, E=0.1,* β^* = 0.1, *Rn= 0.3,* β_1 = 0.4.

5. Conclusions

The peristaltic motion of Bingham plastic fluid in an asymmetric channel with a porous material was examined in this study to determine the impact of magnetism and rotation on it. By choosing peristaltic waves with various ranges, phases, low Reynolds numbers, and wavelengths, the asymmetric duct is created. The expression for the axial velocity, magnetic force, flow function, and current density were also obtained using an application of the perturbation method. Graphs are used to illustrate the findings as follows:

1. Velocity is a decreasing function of the slip parameter β_1 whereas it is a increasing function of the Darcy number Da, rotation Ω and β.
2. The influence of relevant parameters on pumping rate vary depending on the pumping region.
3. The pressure rise enhances above the critical value of flow rate with higher values of Darcy number.
4. For higher values of Ω, Ha and ρ, the size of the trapped bolus decreases while it increases with increasing Da and Rn.

References

[1] H. P, S. V and K. B. R, "Peristaltic transport of non-newtonian fluid in a diverging tube with different wave forms," *Mathematical and Computer Modelling,* vol. 48, no. 7-8, p. 998–1017, 2008.

[2] Rathakrishnan and Ethirajan, "Fluid mechanics," *An introduction. PHI Learning Pvt,* 2022.

[3] Narahari, M and S. S, "Peristaltic transport of a Bingham fluid in contact with a Newtonian fluid," *Int J Appl Math Mech,* vol. 6, no. 11, pp. 41-54, 2010.

[4] S. M. K, "Peristaltic flow of a magneto-micropolar fluid: effect of induced magnetic field," *Journal of Applied Mathematics,* no. 570825, p. 23 pages, 2008.

[5] K. . P. S and K. C. M, "Peristaltic flow of a micropolar fluid through a porous medium in the presence of an external magnetic field," *Communications in Nonlinear Science and Numerical Simulation,* vol. 16, no. 9, p. 3591–3601, 2011.

[6] bdulsalam, I. S, Bhatti and M. M, "The study of non-Newtonian nanofluid with hall and ion slip effects on peristaltically induced motion in a nonuniform channel," *RSC Advances,* vol. 8, no. 15, pp. 904-7915, 2018.

[7] H. T, A. N and A. N, "Peristaltic mechanism of a Maxwell fluid in an asymmetric channel," *Nonlinear Analysis,* vol. 9, no. 4, p. 1474–1490, 2008.

[8] El Misery, E. M. A and F. A. E. K. M, "Effects of a magnetic field on trapping through peristaltic motion for generalized Newtonian fluid in channel," *Physica A: Statistical Mechanics and Its Applications,* vol. 367, pp. 79-92, 2006.

[9] B. D. B, M. G, R. C, . V. H and V. P. K, "Effects of Inclined Magnetic Field and Porous Medium on Peristaltic Flow of a Bingham Fluid with Heat Transfer," *Journal of Applied and Computational Mechanics,* vol. 7, no. 4, p. 1892–1906, 2021.

[10] A. M. Abdulhadi and S. . A. Tamara , "Effect of magnetic field on peristaltic flow of Walters' B fluid through a porous medium in a tapered asymmetric channel," *Journal of advances in Mathematics,* no. 1.12, pp. 6889-6893, 2017.

[11] M. A. Murad and A. M. Ahmed , "Influence of heat and mass transfer on peristaltic transport of viscoplastic fluid in presence of magnetic field through symmetric channel with porous medium," *Journal of Physics,* vol. 1804, no. 1, 2021.